Bose-Einstein Condensate in a Honeycomb Optical Lattice: Fingerprint of Superfluidity at the Dirac Point

Zhu Chen (□□) and Biao Wu (□□)

Phys. Rev. Lett. **107**, 065301 — Published 1 August 2011

DOI: 10.1103/PhysRevLett.107.065301

Bose-Einstein Condensate in a Honeycomb Optical Lattice: Fingerprint of Superfluidity at the Dirac Point

Zhu Chen (陈竹)[1] and Biao Wu (吴飙)[2]

[1]*Institute of Physics, Chinese Academy of Sciences, 100190, Beijing, China*
[2]*International Center for Quantum Materials, Peking University, 100871, Beijing, China*

Mean-field Bloch bands of a Bose-Einstein condensate in a honeycomb optical lattice are computed. We find that the topological structure of the Bloch bands at the Dirac point is changed completely by atomic interaction of arbitrary small strength: the Dirac point is extended into a closed curve and an intersecting tube structure arises around the original Dirac point. These tubed Bloch bands are caused by the superfluidity of the system. Furthermore, they imply the inadequacy of the tight-binding model to describe an interacting Boson system around the Dirac point and the breakdown of adiabaticity by interaction of arbitrary small strength.

PACS numbers: 67.85.Hj, 03.75.Kk, 37.10.Jk,

Inspired by the exciting physics in graphene[1–4], there have been increasing efforts to study ultracold atoms in a honeycomb optical lattice [5–11]. The primary reason is that these ultracold atom systems offer more controlling flexibilities over graphene[12, 13]. For example, with this hexagonal ultracold atom system, one can readily change the lattice strength, tune the atomic scattering strength with Feshbach resonance, and load either bosons or fermions or even a mixture of bosons and fermions in the lattice. There have already been efforts to study conical diffraction[6–8] and observe quantum phases with ultracold bosons in a honeycomb lattice[9]. This controlling flexibility will not only offer deeper insight into the graphene properties but also open up windows for physics beyond graphene.

In this Letter we provide an insight into the interplay between superfluidity and Dirac dynamics by studying a Bose-Einstein condensate (BEC) in a honeycomb optical lattice. To showcase the interplay, we compute the lowest Bloch bands for this BEC system. We find that the topology of the Bloch bands around the Dirac point is completely altered by arbitrary small atomic interaction: an intersecting tube structure appears and the Dirac point is turned into a closed curve. We show that the topological change can be viewed as a permanent fingerprint left in the Bloch bands by superfluidity. As the interaction does not change the Dirac point structure in the tight-binding model, this topological change suggests that the tight-binding model is insufficient to describe the bosonic dynamics in a honeycomb lattice no matter how deep the lattice is. At the same time, these tubed bands imply the breakdown of adiabaticity by arbitrary small atomic interaction. A feasible experimental scheme is suggested to observe this phenomenon.

The honeycomb optical lattice can be experimentally realized by three interfering traveling laser beams[14, 15], and is described mathematically by

$$V(\mathbf{r}) = V_0\Big[\cos(\mathbf{b}_1\cdot\mathbf{r})+\cos(\mathbf{b}_2\cdot\mathbf{r})+\cos((\mathbf{b}_1+\mathbf{b}_2)\cdot\mathbf{r})\Big], \quad (1)$$

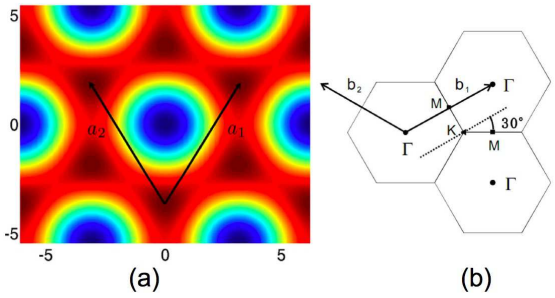

FIG. 1: (color online) (a) Contour map of the hexagonal potential in Eq.(1). The potential well is represented in red and the barrier in blue. The unit vectors are marked as $\mathbf{a}_1$ and $\mathbf{a}_2$. (b) Unit cell in the reciprocal space with unit vectors $\mathbf{b}_1$, $\mathbf{b}_2$ and the high symmetry points $\mathbf{\Gamma}$, $\mathbf{M}$ and $\mathbf{K}$.

where the reciprocal unit vectors $\mathbf{b}_1 = 2\pi(\sqrt{3},1)/(3a)$ and $\mathbf{b}_2 = 2\pi(-\sqrt{3},1)/(3a)$ with $a = 2\lambda_L/3\sqrt{3}$. λ_L is the wavelength of the laser beams. We are interested in the superfluid regime, where the BEC system can be well described by the Gross-Pitaevskii (GP) equation

$$i\hbar\frac{\partial\psi}{\partial t} = -\frac{\hbar^2}{2m}\nabla^2\psi + V(\mathbf{r})\psi + \frac{4\pi\hbar^2 a_s}{m}|\psi|^2\psi. \quad (2)$$

with m the mass of particle and a_s the scattering length. For numerical computation, the above equation is made dimensionless by normalizing the wave function and choosing $6E_R$ as energy unit with $E_R = \hbar^2k_L^2/2m$, $ma^2/\pi^2\hbar$ as the time unit, and $\sqrt{3}a/2\pi$ as the length unit. The scaled nonlinearity and potential strength are denoted as c and v, respectively.

We compute the Bloch wave solutions of the GP equation, which are of the form $\psi_{\mathbf{k}}(\mathbf{r}) = \sum_{m,n} c_{mn}e^{i(\mathbf{k}+\mathbf{G}_{mn})\cdot\mathbf{r}}$ with $\mathbf{G}_{mn} = m\mathbf{b}_1 + n\mathbf{b}_2$, and the corresponding nonlinear Bloch bands. The bands along the high-symmetry point are plotted in Fig.2. Compared to the linear bands in Fig.2(a), we see that the nonlinear bands in (b) have a similar overall structure. However, the part around the Dirac point appears to be modified by nonlinearity.

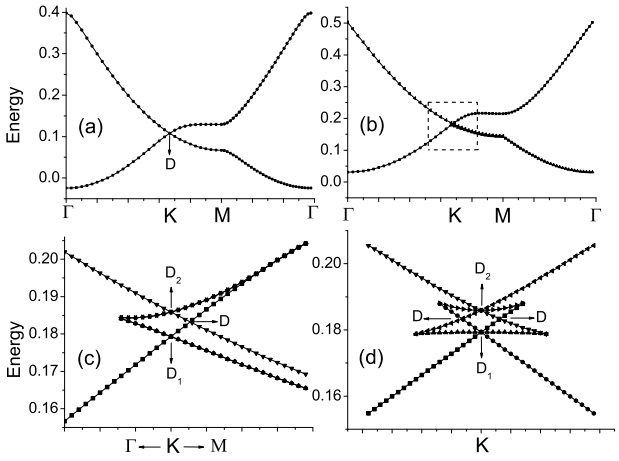

FIG. 2: Bloch bands along the high symmetry points. (a) The linear case. $c = 0$, $v = 0.1$. D marks the Dirac point at point **K**. (b)The nonlinear case. $c = 0.1$, $v = 0.1$. (c) The enlarged rectangle part in (b). There appear two additional crossing points D_1 and D_2 while the linear Dirac point D is shifted away from **K**. (d) The band structure along the direction represented by the dashed line in Fig.1(b).

When it is enlarged, we find in (c) that the two linear bands have split into four bands. As a result, two more additional crossing points D_1 and D_2 appear while the Dirac crossing D is shifted away from point **K**. This feature is also clear in (d), where the Bloch band along the direction 30° off the **K**-**M** axis is plotted. We have also plotted the nonlinear Bloch band near point **M** in Fig.4(b) where we see a loop structure, very similar to the BEC Bloch bands in one dimensional optical lattice[16–18].

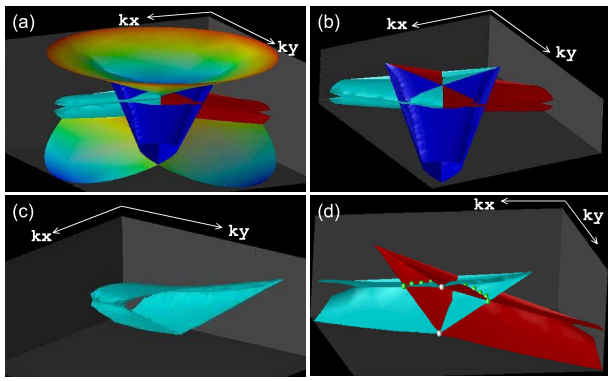

FIG. 3: (color) (a) The lowest nonlinear Bloch bands around point **K**. They consist of three intersecting "tubes", which are sandwiched by two Dirac cones. (b) Three intersecting "tubes", which are aligned along the three **K**-**M** axes; (c) one of three "tubes", whose cross-section area increases monotonically from **M** to **K**; (d) the cross-section of two intersecting "tubes". The white dots are D_1 and D_2 points in Fig.2(c) while the green dots indicate a closed curve where the D point in Fig.2(c) belongs. $v = 0.1, c = 0.1$.

The full BEC Bloch bands near point **K** are plotted in Fig.3(a). The complicated Bloch bands consist of three "tubes", which intersect at point **K** (see Fig.3(b)) and are sandwiched by two Dirac cones. One of the tubes is shown in Fig.3(c): it lies along the **M**-**K** direction and it has a wedged cross-section with an area increasing monotonically from **M** to **K** . Fig.3(d) shows how two tubes intersect. The two white dots mark the top and bottom tips of this intersection and correspond to D_1 and D_2 points in Fig.2(c,d). The green dots indicate part of a closed curve, which results from the intersection of the three tubes; the shifted Dirac point D in Fig.2(c,d) is one of the points on this closed curve. This shows that the Dirac point is turned into a closed curve by the interaction. The three tubes become smaller as the interaction strength c gets weaker. In particular, as c decreases, the tube will disappear first at point **M** and start shrinking toward point **K**. However, surprisingly, the tubes never disappear completely at **K** as long as c is not zero. This indicates that the tubed Bloch bands appear for arbitrary small interaction. Note that the tips of the Dirac cones in Fig.3(a) have only triangular symmetry, and do not have the cylindrical symmetry as in the linear case.

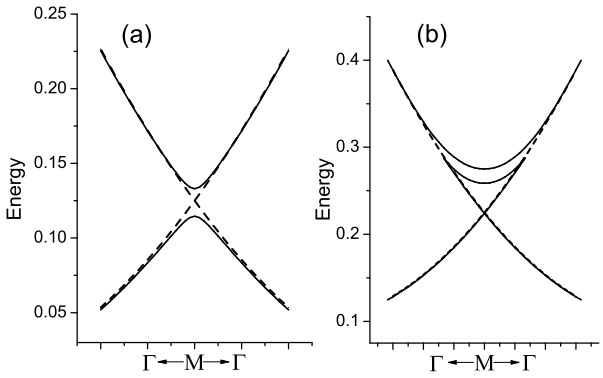

FIG. 4: The lowest Bloch bands for a honeycomb lattice at the **Γ**-**M**-**Γ** branch. (a) Free boson; (b) BEC. The solid curves are Bloch bands while the dashed curves are the energy of the plane waves.

The tubed structure can be viewed as a fingerprint left in the Bloch bands by the superfluidity of the BEC systems. Assume that we have a mass flow of boson particles, which is represented by plane wave $e^{i\mathbf{k}\cdot\mathbf{x}}$ with $\mathbf{k}$ at the Brillouin zone (BZ) edge point **M**. We now slowly turn on an optical lattice of small lattice strength. For free bosons, the flow is stopped by the Brag scattering, the plane wave assumes the form of $\sin(\mathbf{k}\cdot\mathbf{x})$. In the energy band, this is reflected by that the crossing of two plane wave energy bands at **M** is replaced by a gap as seen in Fig.4(a). In the nonlinear case, the situation can be very different: when the interaction is strong so that the superfluid critical velocity is larger than $|\mathbf{k}|$, the small

optical lattice, which can be regarded as perturbation, should not stop the super-flow. This implies that the wave function describing the flow should still resemble the plane wave $e^{i\mathbf{k}\cdot\mathbf{x}}$, and at the same time, the crossing of plane wave energy bands should remain unchanged. This is confirmed by our numerical calculation shown in Fig.4(b). When this superfluidity argument is applied to other points along the BZ edge, we should have a tubed structure seen in Fig.3. In other words, we can view the tubed structure as the fingerprint left in the BEC Bloch bands by superfluidity. For this hexagonal BEC system, this fingerprint stays as long as c is not zero.

We emphasize that the appearance of the tubed structure in the BEC Bloch bands for arbitrary small c is a unique feature for a honeycomb lattice: In one dimensional lattice[16–22] and two dimensional square lattice[23, 24], the looped or tubed nonlinear structure in the Bloch bands appears only when c is bigger than a threshhold value. This unique feature has a profound implication when the tight-binding limit is considered. As is well known, when the lattice is deep, it is believed that the system should be well described by a tight-binding model[25]. However, as shown below, the tight-binding model is not an adequate approximation for a BEC in a honeycomb lattice no matter how deep the lattice is.

Following the usual procedure[10, 25], we write the bosonic field as a sum over the two sub-lattices $\psi = \sum_{\vec{a}} \psi_{\vec{a}} u(\vec{r}-\vec{a}) + \sum_{\vec{b}} \psi_{\vec{b}} u(\vec{r}-\vec{b})$, where $u(\vec{r})$ is the Wannier function and $\vec{a}$ and $\vec{b}$ are lattice vectors in the two sub-lattices, respectively. Then the tight-binding Hamiltonian for our BEC system is

$$H = -\sum_{<\vec{a},\vec{b}>} J_{\vec{\delta}}(\psi^*_{\vec{a}}\psi_{\vec{b}} + \text{h.c.}) + \frac{U}{2}\Big[\sum_{\vec{a}} |\psi_{\vec{a}}|^4 + \sum_{\vec{b}} |\psi_{\vec{b}}|^4\Big], \tag{3}$$

where $J_{\vec{\delta}}$ is the hopping constant with $\vec{\delta}$ indicating three different neighbors and U is the on-site interaction proportional to c. The ground state energy of this Hamiltonian is $E = \pm|\Sigma_1| + U/2$, where $\Sigma_1 = -\sum_{\vec{\delta}} J_{\vec{\delta}} e^{i\mathbf{k}\cdot\vec{\delta}}$. This shows that the interaction has only a trivial effect on the band structure, lifting the Dirac bands by a constant $U/2$. This is very different from the GP equation result, where arbitrary small interaction can destroy the Dirac bands. This surprising difference implies that the tight-binding model can not describe well the BEC system in a honeycomb lattice no matter how deep the lattice is.

After careful analysis, we find that the inadequacy of the tight-binding model may be caused by the inappropriate choice of Wannier function. Let us consider the case where $J_{\vec{\delta}1} = J_{\vec{\delta}2} = J$ and $J_{\vec{\delta}3} > J$[26]. The typical Bloch bands for this case are plotted in Fig. 5, where one immediately notices that the Dirac point is shifted and the bands at point **K** are split, two important features that we also see in Fig.2. To have a different $J_{\vec{\delta}3}$, one needs a set of Wannier functions which have no hexagonal rotational symmetry. This seems to suggest that the choice of Wannier functions, which are used to obtain the tight-binding model, depend on the state of the system. Conventionally, the choice of Wannier functions is independent of the state of the system. To confirm this, more computation needs to be done and will be carried out in the future. One possible way of doing the computation is to use the method proposed in Ref.[27].

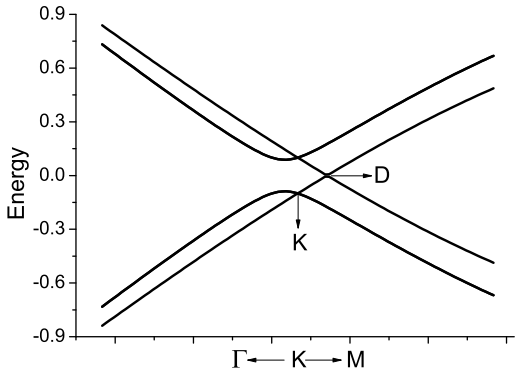

FIG. 5: The linear Bloch bands of the tight-binding model along the **Γ**-**M**-**Γ** branch when $J_{\vec{\delta}1} = J_{\vec{\delta}2} = J$ and $J_{\vec{\delta}3} = 1.1J$. The vertical axis is the energy in the unit of J.

Interestingly, the tubed structure shown in Fig.3 has another important physical implication, the breakdown of adiabaticity by nonlinearity. In the linear case, the state of the system can adiabatically follow the lower left band to the upper right band by passing through the Dirac point. In the nonlinear case, this adiabatic following is broken. This can be seen clearly in Fig.3(d): the system can follow adiabatically passing point D till the tip of the band, where no more band to follow and the adiabaticity is broken. This type of breakdown of adiabaticity is also implied in the loop structure in the one dimensional optical lattice. Such an interesting effect has not only been generalized to general nonlinear quantum systems[28] but also been observed experimentally with ultra-cold atoms[29]. However, the crucial difference of the hexagonal system is that the breakdown of adiabaticity occurs for arbitrary small interaction whereas it happens only when the nonlinearity is bigger than a threshold value in the 1D system or other previously studied systems.

Note that this interesting phenomenon is not limited to the system of BEC in a honeycomb lattice. It can be seen clearly when we approximate this BEC system at point **K** with a three-mode model. The three-mode model is

$$i\frac{\partial}{\partial t}\begin{pmatrix}\phi_1\\ \phi_2\\ \phi_3\end{pmatrix}=\begin{pmatrix}-|\phi_1|^2c-\frac{\delta k_x}{4}-\frac{\sqrt{3}\delta k_y}{4} & v/2 & v/2\\ v/2 & -|\phi_2|^2c+\frac{\delta k_x}{2} & v/2\\ v/2 & v/2 & -|\phi_3|^2c-\frac{\delta k_x}{4}+\frac{\sqrt{3}\delta k_y}{4}\end{pmatrix}\begin{pmatrix}\phi_1\\ \phi_2\\ \phi_3\end{pmatrix}, \quad (4)$$

where δk_x and δk_y denote how much the Bloch wave number $\mathbf{k}$ deviates away from $\mathbf{K}$. This three-mode model can also describe a BEC in a triple-well potential, where the three wells are arranged in a triangular geometry with the depth of each well adjustable[30, 31]. It should also be realizable in experiment with waveguide systems[32–34] and other nonlinear optical systems. This shows that this breakdown of adiabaticity by arbitrary small interaction is general and can happen in a wide range of systems.

Inspired by the experiment in [29], we here propose a scheme to realize the above mentioned triple well configuration. The procedure is as follows. At first, a triangular lattice is formed by three lasers. The triangular potential can be described by $V_{\rm tri} = V_0\left[\cos(x+\frac{y}{\sqrt{3}})+\cos(-x+\frac{y}{\sqrt{3}})+\cos(\frac{2y}{\sqrt{3}})\right]$ with $V_0 < 0$. The second step is to form the triple-well systems by adding a rectangular lattice $V_{\rm rec}(\theta,\varphi) = V_1\left[\cos(x/2+\theta)+\cos(y/\sqrt{3}+\varphi)\right]$ $(V_1 > 0)$. As θ,φ changes, the second optical lattice can not only break the triangular lattice into a series of independent triple-well systems but also change the depth of each well. One should be able to demonstrate the breakdown of adiabaticity by arbitrary small interaction with this triple-well system, similar to the experiment done in Ref. [29].

In sum, we have computed the BEC Bloch bands in a honeycomb optical lattice. Our results show that a tube-intersecting structure can emerge between the up and down Dirac cones for arbitrary small interaction. This structure has two interesting physical implications: (1) the tight-bind model can not describe adequately the BEC in a honeycomb lattice even when the lattice is very deep; (2) the adiabaticity can be broken down by arbitrary small interaction in certain systems. For the latter, we have proposed an experimental scheme to observe it.

We thank Yongping Zhang for useful discussions. We also thank Zhaoxing Liang for the help on numerical calculation. This work was supported by the NSF of China (10825417).

[1] K. S. Novoselov *et al.*, Nature **438**, 197 (2005).
[2] Yuanbo Zhang, Yan-Wen Tan, Horst L. Stormer, and Philip Kim, Nature **438**, 201 (2005).
[3] C. Wu, D. Bergman, L. Balents, and S. DasSarma, Phys. Rev. Lett. **99**, 070401 (2007).
[4] Wang Yao, Shengyuan A. Yang, and Qian Niu, Phys. Rev. Lett. **102**, 096801 (2009).
[5] S. L. Zhu, Baigeng Wang, and L.-M. Duan, Phys. Rev. Lett. **98**, 260402 (2007).
[6] M. J. Ablowitz, S. D. Nixon, and Y. Zhu, Phys. Rev. A **79**, 053830 (2009).
[7] O. Bahat-Treidel, O. Peleg, M. Segev, and H. Buljan, Phys. Rev. A **82**, 013830 (2010).
[8] O. Peleg, G. Bartal, B. Freedman, O. Manela, M. Segev, and D. N. Christodoulides, Phys. Rev. Lett. **98**, 103901 (2007).
[9] Parvis Soltan-Panahi *et al.*, arXiv:1005.1276.
[10] L. H. Haddad and L. D. Carr, cond-mat/1006.3893.
[11] L. H. Haddad and L. D. Carr, Physica D: Nonlinear Phenomena **238**, 1413 (2009).
[12] O. Morsch and M. Oberthaler, Rev. Mod. Phys. **78**, 179 (2006).
[13] V. Yukalov, Laser Physics **19**, 1 (2009).
[14] G. Grynberg, B. Lounis, P. Verkerk, J. Y. Courtois, and C. Salomon, Phys. Rev. Lett. **70**, 2249 (1993).
[15] B. Wunsch, F. Guinea, and F. Sols, New J. Phys. **10**, 103027 (2008).
[16] B. Wu and Q. Niu, New J. Phys. **5**, 104 (2003).
[17] B. Wu and Q. Niu, Phys. Rev. A **61**, 023402 (2000).
[18] M. Machholm, C. J. Pethick, and H. Smith, Phys. Rev. A **67**, 053613 (2003).
[19] B. T. Seaman, L. D. Carr, and M. J. Holland, Phys. Rev. A **71**, 033622 (2005).
[20] B. T. Seaman, L. D. Carr, and M. J. Holland, Phys. Rev. A **72**, 033602 (2005).
[21] E. J. Mueller, Phys. Rev. A **66**, 063603 (2002).
[22] B. P. Venkatesh, J. Larson, and D. H. J. O'Dell, quant-ph/1101.1570.
[23] Z. Chen, Z. Liang, and B. Wu, unpublished.
[24] C.-S. Chien, S.-L. Chang, and B. Wu, Comput. Phys. Commun. **181**, 1727 (2010).
[25] A. Smerzi, A. Trombettoni, P. G. Kevrekidis, and A. R. Bishop, Phys. Rev. Lett. **89**, 170402 (2002).
[26] K. L. Lee, B. Grémaud, R. Han, B.-G. Englert, and C. Miniatura, Phys. Rev. A **80**, 043411 (2009).
[27] B. Wu and J. Shi, arXiv:0907.2046v1.
[28] J. Liu, B. Wu, and Q. Niu, Phys. Rev. Lett. **90**, 170404 (2003).
[29] Y.-A. Chen, S. D. Huber, S. Trotzky, I. Bloch, and E. Altman, Nature Phys. **7**, 61 (2011).
[30] R. Franzosi and V. Penna, Phys. Rev. E **67**, 046227 (2003).
[31] X. Jiang, L.-B. Fu, W.-S. Duan, and J. Liu, to be published.
[32] X. Luo, Q. Xie, and B. Wu, Phys. Rev. A **76**, 051802(R) (2007).
[33] A. Szameit *et al.*, Opt. Lett. **34**, 2700 (2009).
[34] A. S. Desyatnikov *et al.*, Opt. Lett. **32**, 325 (2007).